

Structural diversity of four new metal–organic frameworks with a curved tetracarboxydiimide dicarboxylic acid†

Cite this: *CrystEngComm*, 2014, 16, 834

Huimin Li, Jingmin Zhou, Wei Shi,* Xuejing Zhang, Zhenjie Zhang, Meng Zhang and Peng Cheng*

Four new metal–organic frameworks (MOFs), $\{[\text{Co}_2(\text{L})_2(\text{DMF})_3] \cdot 6.5\text{DMF} \cdot 5\text{H}_2\text{O}\}_n$ (**1**), $\{[\text{Cu}(\text{L})(\text{H}_2\text{O})] \cdot 2\text{DMA}\}_n$ (**2**), $\{[\text{Zn}_2(\text{L})(\text{DMF})_2(\text{HCOO})_2] \cdot 3\text{DMF} \cdot 2\text{H}_2\text{O}\}_n$ (**3**), and $\{[\text{Cd}_2(\text{L})_2(\text{DMF})(\text{H}_2\text{O})(\mu_2\text{-OH}_2)_2] \cdot 3.5\text{DMF} \cdot 2\text{H}_2\text{O}\}_n$ (**4**) ($\text{H}_2\text{L} = N$ -phenyl- N' -phenylbicyclo[2.2.2]oct-7-ene-2,3,5,6-tetracarboxydiimide dicarboxylic acid; DMA = N,N -dimethylacetamide; DMF = N,N -dimethylformamide) have been synthesized under solvothermal conditions. MOFs **1**, **2** and **3** display various interesting two-dimensional (2D) structures, including 2D lattice structure, 2-fold interpenetrated 2D structure, and 2D tube-based network. MOF **4** features an interesting two-fold interpenetrated 3D structure possessing a 6-connected *pcu* network with the point symbol of $\{4^{12} \cdot 6^3\}$. Photoluminescent properties of MOFs **3** and **4** have been investigated in the solid state at room temperature.

Received 7th September 2013,
Accepted 23rd October 2013

DOI: 10.1039/c3ce41805g

www.rsc.org/crystengcomm

Introduction

Metal–organic frameworks (MOFs) have received great attention during the past decades owing to not only their various intriguing structural topologies but also their great potentials as functional materials in magnetism,¹ catalysis,² gas storage/separation,^{3,4} ion exchange,⁵ optical properties,^{6,7} and so on. Although the design and synthesis of such materials are highly influenced by many factors, such as the coordination trend of metal centers, the bridging modes of the ligands, as well as reaction conditions, judicious selection of organic bridging ligands with appropriate symmetry is still an effective approach to construct MOFs with unique structures and properties. Among numerous organic ligands, carboxylic acid ligands, such as 1,4-benzenedicarboxylate and 1,3,5-benzenetricarboxylate,^{8,9} are commonly used in the construction of MOFs due to the coordination diversity of carboxylic group. Based on our previous studies, it is obvious that the coordination modes of ligands with specific symmetry are key factors to the final structures and properties of the products. For example, a series of porous MOFs with high symmetry were successfully obtained using dicarboxylic acid with C_2 -like symmetry such as pyridine-3,5-dicarboxylic acid,¹⁰ pyridine-2,6-dicarboxylic

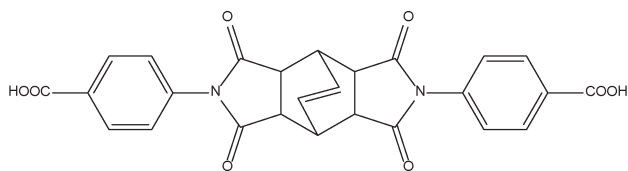
acid,¹¹ 4-hydroxypyridine-2,6-dicarboxylic acid,¹² thiophene-2,5-dicarboxylic acid¹³ and furan-2,5-dicarboxylic acid,¹⁴ which provided an effective “symmetry approach” for the construction of MOFs.

As a continuous work, our attention was paid to a type of curved carboxylic acids with high symmetry as ligand to design and construct new MOFs. N -Phenyl- N' -phenylbicyclo[2.2.2]oct-7-ene-2,3,5,6-tetracarboxydiimide tetracarboxylic acid is an interesting curved and directional ligand in MOFs chemistry.¹⁵ We have designed and constructed a new type of MOF with this ligand showing unusual interpenetrated cationic (MOF- A^+) and anionic (MOF- B^-) nets, as well as ion exchange and luminescent properties.^{15a} N -Phenyl- N' -phenylbicyclo[2.2.2]oct-7-ene-2,3,5,6-tetracarboxydiimide dicarboxylic acid (H_2L) (Scheme 1), similar to the above ligand, was still unexplored in this field. H_2L has specific symmetry within two benzoic acid groups linked at their 4-position by a long curved acid dianhydride, which can be a good candidate for the design and construction of diverse MOFs that deserves further exploration. In this contribution, we report the synthesis and crystal structures of four new MOFs with H_2L . Reactions of H_2L with four transition metal ions generated $\{[\text{Co}_2(\text{L})_2(\text{DMF})_3] \cdot 6.5\text{DMF} \cdot 5\text{H}_2\text{O}\}_n$ (**1**), $\{[\text{Cu}(\text{L})(\text{H}_2\text{O})] \cdot 2\text{DMA}\}_n$ (**2**), $\{[\text{Zn}_2(\text{L})(\text{DMF})_2(\text{HCOO})_2] \cdot 3\text{DMF} \cdot 2\text{H}_2\text{O}\}_n$ (**3**), and $\{[\text{Cd}_2(\text{L})_2(\text{DMF})(\text{H}_2\text{O})(\mu_2\text{-OH}_2)_2] \cdot 3.5\text{DMF} \cdot 2\text{H}_2\text{O}\}_n$ (**4**). The structures of these compounds are significantly influenced by the reaction conditions, such as solvents, metal salt species and ligand–metal ratio. MOFs **1**, **2**, and **3** display different 2D structures, including 2D lattice structure, two-fold interpenetrated 2D lattice structure, and 2D tube-based structure. It is noted that 2D planes of **2** are 2-fold interlinked with each other to

Department of Chemistry, Key Laboratory of Advanced Energy Materials Chemistry (MOE), and Synergetic Innovation Center of Chemical Science and Engineering (Tianjin), Nankai University, Tianjin 300071, PR China.

E-mail: shiwei@nankai.edu.cn, pcheng@nankai.edu.cn

† Electronic supplementary information (ESI) available: PXRD spectra and TGA spectra. CCDC 951691–951694. For ESI and crystallographic data in CIF or other electronic format see DOI:10.1039/c3ce41805g



Scheme 1 The structure of H_2L .

provide an unusual interpenetrated double layer. 2D tube-based structure of **3** is also rare in coordination chemistry. In addition, MOF **4** presents an interesting two-fold interpenetrated 3D framework. The luminescent properties of **3** and **4** were also studied.

Experimental section

Materials and instrumentation

All the reagents and solvents employed were commercially available and used without further purification. Elemental analyses (C, H, and N) were performed on a Perkin-Elmer 240 CHN elemental analyzer. IR spectra were recorded in the range 400–4000 cm^{-1} on a Bruker TENOR 27 spectrophotometer using KBr pellets. Powder X-ray diffraction measurements were recorded on a D/Max-2500 X-ray diffractometer using $\text{Cu K}\alpha$ radiation. The luminescent spectra were measured on a Varian Cary Eclipse fluorescence spectrophotometer. Thermal analyses (under nitrogen atmosphere, heating rate of 10 $^\circ\text{C min}^{-1}$) were carried out in a Labsys NETZSCH TG 209 Setaram apparatus. The $^1\text{H-NMR}$ spectrum was measured on a Mercury Vx-300 NMR spectrometer.

Synthesis of H_2L

A mixture of 20 mmol (2.7400 g) 4-aminobenzoic acid and 10 mmol (2.4800 g) bicyclo[2.2.2]oct-7-ene-2,3,5,6-tetracarboxylic acid dianhydride was added into 100 mL acetic acid. Then the mixture was heated to reflux for 12 h. White powder was obtained by filtration, washing, and drying. H_2L was used without further purification. Element analysis (%) found (calcd.) for H_2L ($\text{C}_{26}\text{H}_{18}\text{O}_8\text{N}_2$), C 63.85 (64.20), H 4.02 (3.73), N 5.78 (5.76). IR bands (KBr , v/cm^{-1}) for H_2L : 2937 (m), 1709 (vs), 1607 (m), 1513 (m), 1381 (s), 1285 (m), 1178 (s), 858 (w), 798 (m), 766 (m), 717 (m). $^1\text{H-NMR}$ (300 MHz, DMSO-d_6), δ (ppm): 3.45 (s, 2H), 3.52 (s, 1H), 6.31 (t, 1H), 7.30 (d, 2H) 7.99 (d, 2H).¹⁶

Synthesis of $\{[\text{Co}_2(\text{L})_2(\text{DMF})_3]\cdot 6.5\text{DMF}\cdot 5\text{H}_2\text{O}\}_n$ (**1**)

The mixture of H_2L (0.10 mmol, 0.0486 g), $\text{CoCl}_2\cdot 6\text{H}_2\text{O}$ (0.25 mmol, 0.0595 g), $\text{LiOH}\cdot\text{H}_2\text{O}$ (0.2 mmol, 0.0839 g) and 2 mL DMF was sealed in a 25 mL Teflon-lined autoclave. After being heated at 80 $^\circ\text{C}$ for 3 days, it was cooled to room temperature at a rate of 2 $^\circ\text{C h}^{-1}$. Red block crystals were obtained (yield: 33% based on Co). Element analysis (%) found (calcd.) for $\text{C}_{80.5}\text{H}_{108.5}\text{Co}_2\text{N}_{13.5}\text{O}_{30}$ (**1**), C 51.64 (51.67), H 5.92 (5.84), N 9.89 (10.10); IR (KBr , v/cm^{-1}): 3371 (br), 2935.26 (w), 1773 (m), 1711 (vs), 1661 (s), 1602 (s), 1556 (s), 1508 (m), 1387

(vs), 1299 (m), 1191 (s), 1104 (m), 1015 (w), 770 (s), 725 (m), 699 (m), 602 (m).

Synthesis of $\{[\text{Cu}(\text{L})(\text{H}_2\text{O})]\cdot 2\text{DMA}\}_n$ (**2**)

The mixture of H_2L (0.10 mmol, 0.0486 g), $\text{CuCl}_2\cdot 6\text{H}_2\text{O}$ (0.25 mmol, 0.0606 g), 0.5 mL ethanol and 3 mL DMA was sealed in a 25 mL Teflon-lined autoclave. The mixture was heated to 80 $^\circ\text{C}$ for 3 days, and then cooled to room temperature at a rate of 2 $^\circ\text{C h}^{-1}$. Blue rhombic block crystals were obtained (yield: 55%, based on Cu). Element analysis (%) found (calcd.) for $\text{C}_{34}\text{H}_{36}\text{CuN}_4\text{O}_{11}$ (**2**), C 54.87 (55.16), H 5.06 (4.90), N 8.03 (7.67); IR (KBr , v/cm^{-1}): 3471 (m), 2945 (m), 1707 (vs), 1599 (vs), 1512 (s), 1406 (vs), 1303 (w), 1191 (s), 1016 (m), 837 (w), 800 (s), 769 (vs), 735 (s), 595 (m), 538 (w), 472 (w), 424 (w).

Synthesis of $\{[\text{Zn}_2(\text{L})(\text{DMF})_2(\text{HCOO})_2]\cdot 3\text{DMF}\cdot 2\text{H}_2\text{O}\}_n$ (**3**)

The mixture of H_2L (0.10 mmol, 0.0486 g), $\text{Zn}(\text{ClO}_4)_2\cdot 6\text{H}_2\text{O}$ (0.10 mmol, 0.0372 g), $\text{LiOH}\cdot\text{H}_2\text{O}$ (0.2 mmol, 0.0839 g) and 3 mL DMF was sealed in a 25 mL Teflon-lined autoclave. The mixture was heated to 80 $^\circ\text{C}$ for 3 days, and then cooled to room temperature at a rate of 2 $^\circ\text{C h}^{-1}$. Colorless prism crystals were obtained (yield: 60% based on Zn). Element analysis (%) found (calcd.) for $\text{C}_{43}\text{H}_{57}\text{Zn}_2\text{N}_7\text{O}_{19}$ (**3**), C 46.58 (46.67), H 5.09 (5.19), N 9.20 (8.86); IR (KBr , v/cm^{-1}): 3457 (br), 1713 (vs), 1659 (s), 1607 (m), 1558 (m), 1508 (w), 1338 (s), 1300 (w), 1194 (m), 1102 (m), 1018 (w), 843 (w), 770 (m), 728 (w), 600 (w).

Synthesis of $\{[\text{Cd}_2(\text{L})_2(\text{DMF})(\text{H}_2\text{O})(\mu_2\text{-OH})_2]\cdot 3.5\text{DMF}\cdot 2\text{H}_2\text{O}\}_n$ (**4**)

The mixture of H_2L (0.10 mmol, 0.0486 g), $\text{CdCl}_2\cdot 6\text{H}_2\text{O}$ (0.25 mmol, 0.0729 g), 0.5 mL methanol and 3 mL DMF was sealed in a 25 mL Teflon-lined autoclave. The mixture was heated to 80 $^\circ\text{C}$ for 3 days, and then cooled to room temperature at a rate of 2 $^\circ\text{C h}^{-1}$. Colorless block crystals were obtained (yield: 42% based on Cd). Element analysis (%) found (calcd.) for $\text{C}_{65.5}\text{H}_{73.5}\text{Cd}_2\text{N}_{8.5}\text{O}_{25.5}$, C 48.72 (48.78), H 4.53 (4.59), N 7.87 (7.38); IR (KBr , v/cm^{-1}): 3459 (br), 2934 (w), 1772 (w), 1715 (vs), 1661 (vs), 1604 (vs), 1558 (s), 1508 (m), 1390 (vs), 1299 (m), 1192 (s), 1102 (m), 929 (w), 771 (s), 728 (m), 408 (w).

X-ray crystallography

Data collections of **1–4** were performed on an Oxford SuperNova TM diffractometer with graphite-monochromated $\text{Mo-K}\alpha$ radiation ($\lambda = 0.71073 \text{ \AA}$) using ω -scan technique at 150 K. The structures were solved by direct methods and refined with the full matrix least-squares technique based on the SHELXS-97 and SHELXL-97 programs.¹⁷ Anisotropic thermal parameters were assigned to all non-hydrogen atoms. The hydrogen atoms of the organic ligand were generated geometrically; the hydrogen atoms of the water molecules were located from difference maps and refined with isotropic temperature factors.

The contributions of disordered solvent molecules in **1–4** were treated as diffuse using the squeeze procedure in Platon.¹⁸ Details for structural analysis are summarized in Table 1.

Table 1 Data collection and processing parameters for 1–4

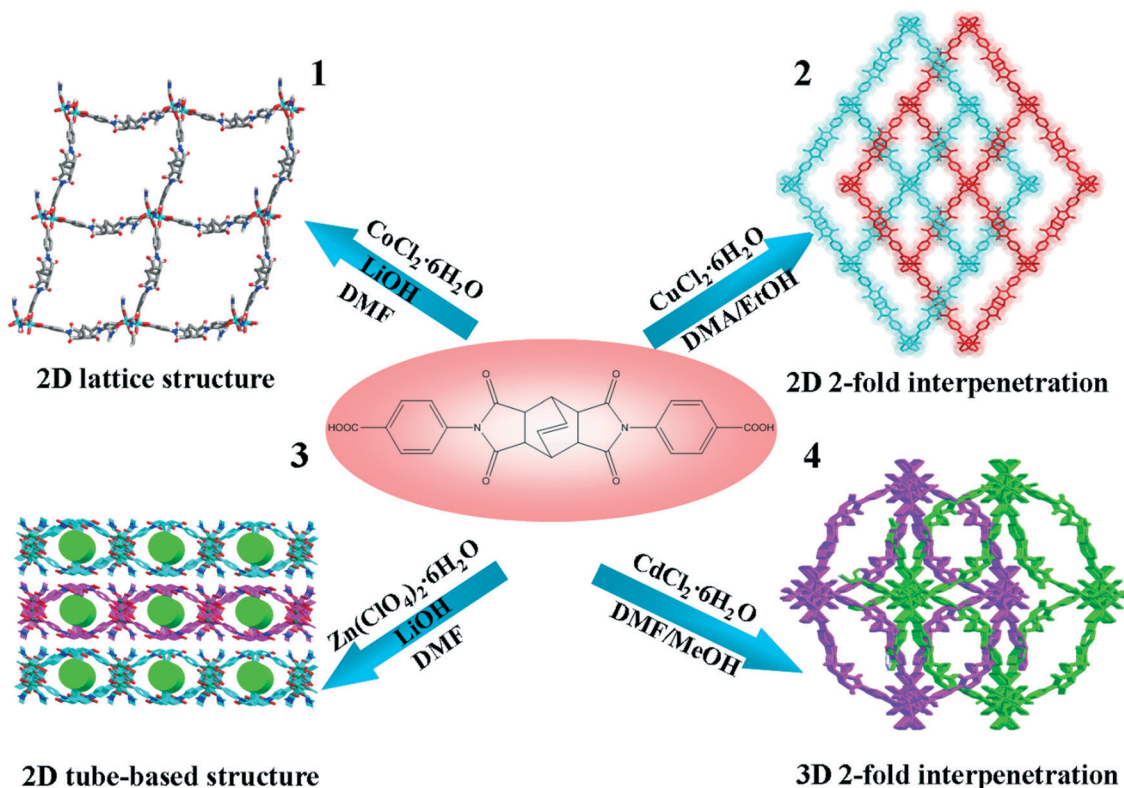
Compounds	1	2	3	4
Formula	C ₆₁ H ₅₃ Co ₂ N ₇ O ₁₉	C ₃₄ H ₃₆ CuN ₄ O ₁₁	C ₄₃ H ₅₇ Zn ₂ N ₇ O ₁₉	C _{65.5} H _{73.5} Cd ₂ N _{8.5} O _{25.5}
Fw	1305.96	740.21	1106.77	1612.65
Temp, K	293(2)	293(2)	293(2)	293(2)
Crystal system	Triclinic	Orthorhombic	Orthorhombic	Monoclinic
Space group	<i>P</i> $\bar{1}$	<i>Ibam</i>	<i>Pcca</i>	<i>P2/c</i>
<i>a</i> , Å	11.4985(3)	11.744(2)	11.7133(3)	15.1796(7)
<i>b</i> , Å	21.2760(6)	19.878(4)	18.7995(5)	15.6453(5)
<i>c</i> , Å	21.4387(6)	36.094(7)	24.1755(6)	16.9845(15)
α , °	77.071(2)	90	90	90
β , °	80.672(2)	90	90	119.218(5)
γ , °	88.411(2)	90	90	90
<i>V</i> , Å ³	5044.0(2)	8426(3)	5223.5(2)	3520.3(4)
<i>Z</i>	2	8	8	2
<i>D</i> _c , g cm ⁻³	0.860	0.889	1.227	1.242
μ , mm ⁻¹	0.377	0.553	0.965	0.668
<i>R</i> _{int}	0.0304	0.0954	0.0480	0.0444
GOF on <i>F</i> ²	0.922	1.044	1.053	1.069
<i>R</i> ₁ , <i>wR</i> ₂ [<i>I</i> > 2 σ (<i>I</i>)]	0.0565, 0.1683	0.0793, 0.2198	0.0629, 0.1713	0.0867, 0.2439
<i>R</i> ₁ , <i>wR</i> ₂ (all data)	0.0756, 0.1788	0.1248, 0.2488	0.0812, 0.1834	0.1062, 0.2622
$\Delta\rho_{\text{max/min}}$ (e Å ⁻³)	1.436/−0.592	0.536/−0.349	1.03/−0.71	2.03/−1.11

Results and discussion

Synthesis and structures

MOFs 1–4 were generated by solvothermal reaction of H₂L with different transition metal salts (Co^{II}, Cu^{II}, Zn^{II} and Cd^{II} salts), and the synthetic strategies of 1–4 were presented in Scheme 2. In general, the reaction variables (solvent,

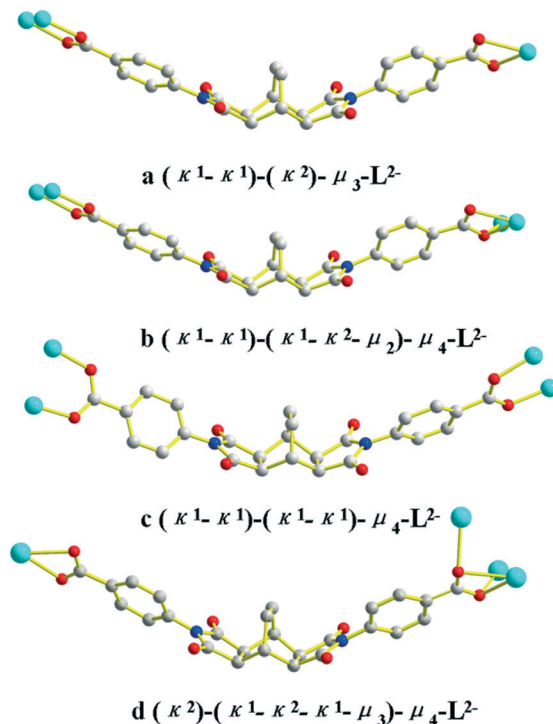
pH value, metal salts species, temperature, and time of reaction, *etc.*) can influence the reaction process and the final products. Solvent as template is one of the keys to the construction of MOFs because solvent can act as space-filling molecules.¹⁹ For MOFs 1, 3 and 4, DMF solvents behave as not only coordinated molecules but also crystal lattice molecules. For MOF 2, one water molecule coordinates with Cu²⁺

**Scheme 2** Synthesis schematic diagrams for 1–4.

and free DMA molecules act as space-filling solvents. pH value is another important factor to construct MOFs. Without LiOH·H₂O, 2D two-fold interpenetrated 2 and 3D two-fold interpenetrated 4 were obtained. The difference of transition metal ions also plays an essential role in the construction of the compounds. The diverse connection modes of the secondary building units (SBUs) are due to the coordination trend of the central metal ions, and further leads to the different structures. For 1, two six-coordinated Co^{II} ions are three-fold connected by carboxyl groups to form a dinuclear secondary building units (SBUs) and adjacent dinuclear Co-SBUs are linked through L²⁻ to generate 2D lattice structure. For 2, each dinuclear Cu^{II} paddle-wheel SBU is connected with adjacent four Cu^{II} SBUs through L²⁻ to generate a 2D rhombic layer as well. However, different from 1, MOF 2 presents an interesting interpenetrating network due to the diversity of metal ions and pH value. For 3, four-coordinated and six-coordinated Zn^{II} ions are alternately connected with each other through carboxyl groups to form a 1D chain and these chains are connected by L²⁻ generating a 2D structure with 1D tube-shape channels. For 4, Cd^{II} ions adopt six-coordinated and eight-coordinated modes forming a trinuclear Cd₃ SBU and these Cd₃ SBUs in a line are linked by μ₂-OH₂ to Cd^{II} chains, which are further connected with each other by L²⁻ from different directions to generate a two-fold interpenetrated 3D structure.

Crystal structure of {[Co₂(L)₂(DMF)₃·6.5DMF·5H₂O]_n (1)

1 belongs to triclinic space group *P* $\bar{1}$. There are two crystallographically independent six-coordinated Co^{II} ions (Co1 and Co2), two L²⁻, three DMF molecules in the asymmetric unit (Fig. 1a). Co1 coordinates with six oxygen atoms from three carboxylic oxygen atoms (O1A, O2A, and O4) of (κ¹-κ¹)-(κ²)-μ₃-L²⁻ (Scheme 3a) and other three carboxylic oxygen atoms (O9, O10, and O16B) of (κ¹-κ¹)-(κ¹-κ²-μ₂)-μ₄-L²⁻ (Scheme 3b). Co2 adopts a slightly distorted octahedral coordination geometry with three carboxylic oxygen atoms from one (κ¹-κ¹)-(κ²)-μ₃-L²⁻ (O3) and two (κ¹-κ¹)-(κ¹-κ²-μ₂)-μ₄-L²⁻



Scheme 3 The coordination modes of H₂L in 1-4.

(O9 and O15A), and other three oxygen atoms from DMF molecules. The Co-O bond lengths are in the range of 1.995(2)–2.228(3) Å. Co1 and Co2 are three-fold bridged by two (κ¹-κ¹)-carboxylic groups (O3 and O4, O15A and O16B) and one (κ¹-κ²-μ₂)-carboxylic group (O9 and O10) to form a dinuclear SBU. These Co-SBUs are connected through (κ¹-κ¹)-(κ²)-μ₃-L²⁻ along *b* axis and (κ¹-κ¹)-(κ¹-κ²-μ₂)-μ₄-L²⁻ along *c* axis to generate a 2D lattice structure along *a* axis (Fig. 1b). The 2D planes are pile-up of dislocations to form a 3D supramolecular structure through weak intermolecular interaction of π···π dislocated stacking (Fig. 1c).

Crystal structure of {[Cu(L)(H₂O)]·2DMA}_n (2)

MOF 2 crystallizes in orthorhombic space group *Ibam*. As shown in Fig. 2, there are one crystallographically independent Cu^{II} ions, one L²⁻ and one water molecules in the asymmetric unit. Cu^{II} ion is five-coordinated with four carboxylic oxygen atoms (O1, O1A, O2B, and O2C) from (κ¹-κ¹)-(κ¹-κ¹)-μ₄-L²⁻ (Scheme 3c) and one water molecule (Fig. 2a). The Cu-O bond lengths range from 1.940(3) to 2.131(6) Å. Two adjacent Cu^{II} ions are linked with four (κ¹-κ¹)-carboxylic groups to form binuclear SBUs of square paddlewheels, which are further linked by (κ¹-κ¹)-(κ¹-κ¹)-μ₄-L²⁻ to build a 2D plane with rhombic lattices (Fig. 2b). Each 2D layer has an undulating net with rhombic windows, in which each dinuclear Cu^{II} paddle-wheel SBU connects with four neighboring SBUs by the curved ligands. It is notable that, different from 1, two (4,4) nets are interlinked with each other to generate a parallel interpenetrated 2D layer (Fig. 2c). Although the

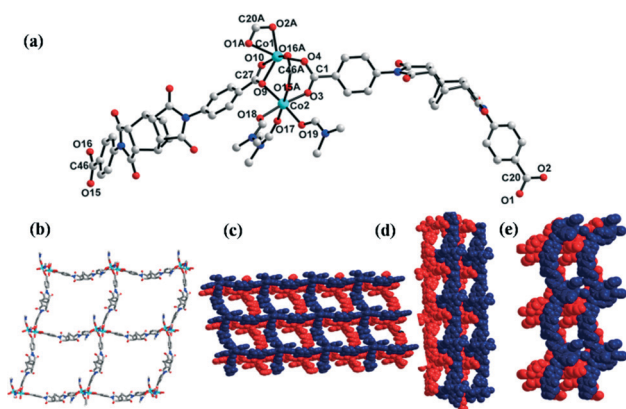


Fig. 1 (a) The coordination environment of MOF 1 (H atoms and solvent molecules were omitted for clarity), (b) the 2D lattice structure along *a*-axis, (c) the packing diagram along *a*-axis, (d) the packing diagram along *b*-axis, (e) the packing diagram along *c*-axis.

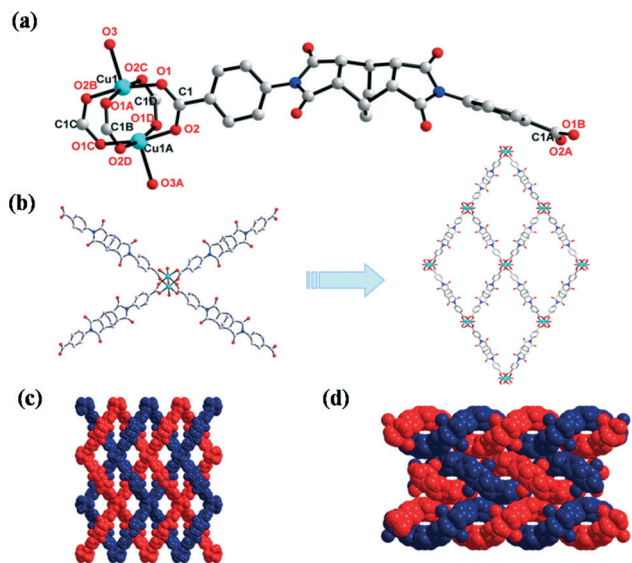


Fig. 2 (a) The coordination environment of MOF 2 (H atoms and solvent molecules were omitted for clarity), (b) the 2D rhombic plane viewed along *a*-axis, (c) two-fold interpenetration viewed along the *b*-axis, and (d) the staking diagram along *c*-axis.

formation of structurally interpenetrated networks is hardly prospective and is obtained rather accidentally, such a parallel interpenetrated 2D layer is interesting and rather rare. The reported parallel interpenetrated 2D compounds with (4,4) nets tend to adopt a single metal ion as a node to connect with four ligands,²⁰ while 2 adopts dinuclear Cu^{II} paddle-wheel SBUs linked with each other by four L²⁻.

Though the main networks of MOFs 1 and 2 are similar, the packing modes of the networks are totally different. In MOF 1, each Co₂ SBU is linked with four curved L²⁻, and the curved L²⁻ ligands along the same direction are bent consistently, while the L²⁻ along different directions are bent oppositely. In MOF 2, the contrary is the case. L²⁻ along the same direction linked to one Cu₂ SBU are bent in opposite directions. As a result, the 2D networks of 1 tend to pile-up of dislocations (*i.e.* interdigitation) and those of 2 prefer to interpenetrate as a double layer so that they can minimize the systematic energy through optimal filling of the space. In addition, MOFs 1 and 2 show two ways in which a crystal can maximize its packing efficiency interdigitation and interpenetration. It is also noted that interdigitation and interpenetration are caused by different bent directions of the same ligand, which is not reported up to date, to the best of our knowledge.

Crystal structure of $\{[\text{Zn}_2(\text{L})(\text{DMF})_2(\text{HCOO})_2] \cdot 3\text{DMF} \cdot 2\text{H}_2\text{O}\}_n$ (3)

Single crystal X-ray analyses reveal that 3 crystallizes in orthorhombic space group *Pcca*. As shown in Fig. 3a, there are two crystallographically independent Zn^{II} ions (Zn1 and Zn2), one L²⁻, two DMF and two HCOO⁻ in the asymmetric unit. Zn1 is four-coordinated with two carboxylic oxygen atoms (O5 and O5A) from two (κ¹-κ¹)-(κ¹-κ¹)-μ₄-L²⁻ (Scheme 3c) and two formate oxygen atoms (O1 and O1A), forming slightly distorted

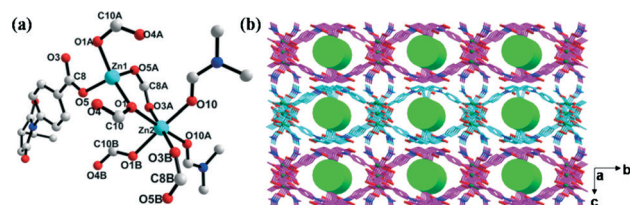


Fig. 3 (a) The coordination environment of MOF 3 (H atoms and solvent molecules were omitted for clarity), (b) the 3D supermolecular network.

tetrahedral coordination geometry. The formate groups were generated by the decomposition of DMF.²¹ Zn₂ is six-coordinated with two carboxylic oxygen atoms (O3A and O3B) from two (κ¹-κ¹)-(κ¹-κ¹)-μ₄-L²⁻, two formate oxygen atoms (O1 and O1B) and two oxygen atoms (O10 and O10A) from two DMF molecules to form octahedral coordination geometry. The Zn–O bond lengths vary from 1.957(5) to 2.138(5) Å. Zn1 and Zn2 are connected by two (κ¹-κ¹)-carboxylic oxygen atoms and (κ¹-μ₂)-formate oxygen atoms forming a binuclear SBU. Adjacent binuclear SBUs are connected by (κ¹-κ¹)-carboxylic groups and formate groups to form 1D chains, which are further linked by L²⁻ ligands to a 2D layer. The weak interactions of π⋯π stacking between adjacent layers generate a 3D supermolecular network with 1D tube-shape channel along *a* axis with the dimensions of *ca.* 9.8 Å × 15.3 Å, which is produced by two L²⁻ curved in opposite directions connected with Zn₂ (Fig. 3b). The channels are occupied by water and DMF molecules. PLATON¹⁸ analysis reveals that the structure contains voids of 1229.5 Å³, which represents 23.1% volume per unit cell with the removal of water and DMF molecules. As far as we know, 2D tube-based plan structure is still unexplored, although 2D square-grid structure and MOFs with 1D tube-shape channel are known.²²

Crystal structure of $\{[\text{Cd}_2(\text{L})_2(\text{DMF})(\text{H}_2\text{O})(\mu_2\text{-OH}_2)_2] \cdot 3.5\text{DMF} \cdot 2\text{H}_2\text{O}\}_n$ (4)

MOF 4 crystallizes in monoclinic space group *P2/c* and exhibits an interesting two-fold interpenetrating 3D structure. There are two crystallographically independent Cd^{II} ions (Cd1 and Cd2), one L²⁻, one DMF molecule, and three water molecules in the asymmetric unit, as shown in Fig. 4a. Cd1 is coordinated with eight oxygen atoms from two (κ²)-carboxylic groups (O7A, O8A, O7B, and O8B) and two (κ¹-κ²-κ¹-μ³)-carboxylic groups (O1, O2, O1A, and O2A) of (κ²)-(κ¹-κ²-κ¹-μ³)-μ₄-L²⁻ (Scheme 3d), and the coordination geometry of Cd1 ion can be viewed as a distorted trigonal dodecahedron. Cd2 is six-coordinated adopting octahedral coordination geometry with two carboxylic oxygen atoms (O1 and O2A) from (κ²)-(κ¹-κ²-κ¹-μ³)-μ₄-L²⁻, two μ₂-OH₂ molecules (O9 and O9A), one water molecule, and one DMF molecule. The Cd–O bond lengths are in the range of 2.276–2.543 Å. Cd1 is connected with two Cd2 by two (κ¹-κ²-κ¹-μ³)-carboxylic groups forming a trinuclear Cd₃ SBU, and adjacent trinuclear SBUs are linked by two μ₂-OH₂

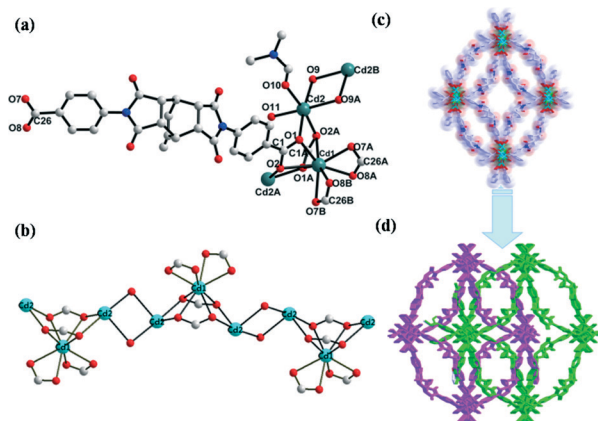


Fig. 4 (a) The coordination environment of MOF 4 (H atoms and solvent molecules were omitted for clarity), (b) 1D chain, (c) the 3D framework, and (d) the two-fold interpenetrated structure.

atoms to an one-dimensional (1D) Cd₃ chain (Fig. 4b). Furthermore, 1D Cd₃ chains are linked by $(\kappa^2)-(\kappa^1-\kappa^2-\kappa^1-\mu_3)-\mu_4-L^2-$ along different directions into a beautiful three-dimensional (3D) network. Two sets of such 3D networks are interpenetrated with each other by weak interactions of $\pi \cdots \pi$ stacking to form a two-fold interpenetrated structure (Fig. 4c). In order to simplify this complicated framework, the network topology has been analyzed by the freely available computer program TOPOS.²³ If each trinuclear Cd₃ SBU is considered as a six-connected node which links with four ligands and another two Cd₃ SBUs by μ_2-OH_2 , and all the ligands and μ_2-OH_2 serve as bridging linkers, the structure can be considered as a 6-connected net named **pcu** (Fig. 5). The point symbol of the topology can be expressed as $\{4^{12} \cdot 6^3\}$. Among the two-fold interpenetrated structures based on 3D networks, MOFs based on 6-connected octahedral nodes and linear linkers are rarely observed.²⁴

Powder X-ray diffraction (PXRD) and thermal gravimetric analyses (TGA)

To confirm the phase purity of the four new compounds, PXRD patterns have been carried out at room temperature (Fig. S1, ESI[†]). The peak positions of the experimental PXRD

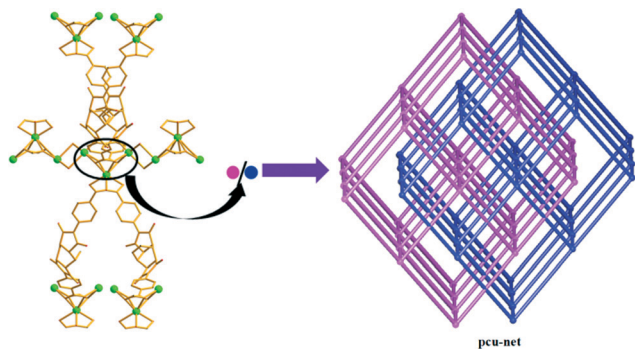


Fig. 5 The two-fold interpenetrated topological diagram of 4 (Cd₃ SBU: 6-connected node).

are well in agreement with the simulated data, demonstrating the phase purity of the compounds.

The thermal stabilities of 1–4 were measured by TGA in N₂ atmosphere from 25 to 800 °C (Fig. S2, ESI[†]). For 1, a weight loss of 41.83% from 25 to 239.5 °C was observed, corresponding to the loss of three coordinated DMF molecules, five water molecules and six and half DMF molecules in the lattice (theoretical 41.90%). With increasing the temperature to 400 °C, the structure began to decompose, illustrating the strong thermal stability of 1. For 2, a weight loss of 23.35% from 25 to 340.5 °C was observed, corresponding to the release of two free DMA (theoretical 23.54%), then the framework decomposed upon further heating. For 3, the first weight loss of 22.61% occurred in the temperature ranging from 25 to 339.6 °C due to the loss of three lattice DMF and two lattice water molecules (theoretical 22.99%), and further heating led to the decomposition of ligands. MOF 4 displayed a weight loss of 18.21% between 25 °C and 213.0 °C, which is in accordance with the loss of lattice solvent molecules (3.5DMF and 2H₂O, theoretical 18.07%). With increasing the temperature to 268.3 °C, the second weight loss of 3.85%, which accords with the loss of three coordinated water molecules (theoretical 3.35%). On further heating, sharp weight loss was observed, indicating the decomposition of the organic ligands.

Luminescent properties

Although a lot of transition metal ions have been used to construct MOFs, the Zn and Cd-based MOFs are the most interested transition-metal-based luminescent MOFs. The d¹⁰ metal ions not only have various coordination numbers and geometries, but also display luminescent properties when coordinated with functional ligands.²⁵ The photoluminescent properties of MOFs 3 and 4 have been studied in the solid state at room temperature, as shown in Fig. 6. The strongest emission peak at 333 nm for H₂L ligand is observed upon excitation at 270 nm. This emission band can be attributed to $\pi^*-\pi$ or π^*-n transitions.²⁶ Excitation of the as-synthesized 3 at 340 nm leads to the maximum emission peak at 408 nm.

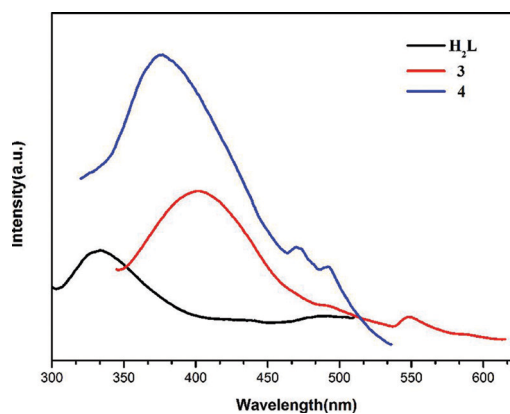


Fig. 6 The solid-state emission spectra of H₂L, 3, and 4.

Upon excitation at 328 nm the maximum emission peaks of 4 are observed at 377 nm. On comparison with the free H₂L ligand, the maximum emission peak of 3 shows a red shift of 75 nm and that of 4 shows a red shift of 44 nm. Considering that Zn^{II} ions and Cd^{II} ions are difficult to oxidize or reduce due to their d¹⁰ configuration, the emissions of MOFs 3 and 4 are neither metal-to-ligand charge transfer (MLCT) nor ligand-to-metal charge transfer (LMCT) in nature,²⁷ which are mainly based on the luminescence of ligands.²⁸ The photoluminescent of 3 and 4 may originate from the intraligand $\pi^*-\pi$ or $\pi^*-\text{n}$ transition of the H₂L ligand that is modified by the Zn^{II} and Cd^{II} ions. Different coordination environments may be an important factor on influencing different luminescent behaviours of 3 and 4.

Conclusion

In summary, we have successfully synthesized four new MOFs with an interesting curved dicarboxylic ligand. MOFs 1, 2, and 3 display various 2D structures, including 2D lattice structure, two-fold 2D interpenetrated lattice, and tube-based 2D network, respectively. MOF 4 shows an interesting two-fold interpenetrated 3D structure possessing a 6-connected pcu topology with the point symbol of {4¹².6³}. The differences in the reaction conditions have played an important role on the structural diversity of 1–4. The luminescent measurements of 3 and 4 indicate that different coordination environments of d¹⁰ ions (Zn^{II} or Cd^{II}) influence the luminescent properties of the ligands. This work illustrates a promising approach to rational design and synthesis of MOFs with long curved dicarboxylates ligands and more effort is being focused on porous and functional MOFs with diverse structures based on this curved dicarboxylate ligand.

Acknowledgements

We thank the “973 program” (2012CB821702), the NSFC (21373115 and 21331003) and MOE (20120031130001) for financial support.

Notes and references

- (a) D. Pierre and R. L. Jeffrey, *Chem. Soc. Rev.*, 2011, **40**, 3249; (b) K. Mohamedally, *Chem. Soc. Rev.*, 2009, **38**, 1353; (c) N. W. Ockwig, O. Delgado-Friedrichs, M. O’Keeffe and O. M. Yaghi, *Acc. Chem. Res.*, 2005, **38**, 176; (d) H. L. Gao, B. Zhao, X. Q. Zhao, Y. Song, P. Cheng, D. Z. Liao and S. P. Yan, *Inorg. Chem.*, 2008, **47**, 11057; (e) M. H. Zeng, B. Wang, X. Y. Wang, W. X. Zhang, X. M. Chen and S. Gao, *Inorg. Chem.*, 2006, **45**, 7069; (f) D. Sun, D. J. Collins, Y. Ke, J. L. Zuo and H. C. Zhou, *Chem.–Eur. J.*, 2006, **12**, 3768; (g) Y. X. Ke, D. J. Collins, D. F. Sun and H. C. Zhou, *Inorg. Chem.*, 2006, **45**, 1897.
- (a) Y. L. Jeong, K. F. Omar, R. John, A. S. Karl, T. N. SonBinh and T. H. Joseph, *Chem. Soc. Rev.*, 2009, **38**, 1450; (b) L. Q. Ma, A. Carter and W. B. Lin, *Chem. Soc. Rev.*, 2009, **38**, 1248; (c) Y. K. Hwang, D. Y. Hong, J. S. Chang, S. H. Jhung, Y. K. Seo, J. Kim, A. Vimont, M. Daturi, C. Serre and G. Férey, *Angew. Chem., Int. Ed.*, 2008, **47**, 4144; (d) D. N. Dybtsev, A. L. Nuzhdin, H. Chun, K. P. Bryliakov, P. Konstantin, E. P. Talsi, V. P. Fedin and K. Kim, *Angew. Chem.*, 2006, **118**, 930; (e) C. D. Wu, A. Hu, L. Zhang and W. B. Lin, *J. Am. Chem. Soc.*, 2005, **127**, 8940; (f) C. D. Wu, A. Hu, L. Zhang and W. Lin, *J. Am. Chem. Soc.*, 2005, **127**, 8940; (g) J. S. Seo, D. Whang, H. Lee, S. I. Jun, J. Oh, Y. J. Jeon and K. Kim, *Nature*, 2000, **404**, 982.
- (a) T. M. McDonald, W. R. Lee, J. A. Mason, B. M. Wiers, C. S. Hong and J. R. Long, *J. Am. Chem. Soc.*, 2012, **134**, 7056; (b) P. S. Myunghyun, J. P. Hye, K. P. Thazhe and D. W. Lim, *Chem. Rev.*, 2012, **112**, 782; (c) J. Kang, S. H. Wei and Y. H. Kim, *J. Am. Chem. Soc.*, 2010, **132**, 1510; (d) A. W. Thornton, K. M. Nairn, J. M. Hill, A. J. Hill and M. R. Hill, *J. Am. Chem. Soc.*, 2009, **131**, 10662; (e) B. Kesanli, Y. Cui, M. Smith, E. Bittner, B. Bockrath and W. Lin, *Angew. Chem.*, 2005, **117**, 74; (f) B. L. Chen, M. Eddaoudi, S. T. Hyde, M. O. Keffe and O. M. Yaghi, *Science*, 2001, **291**, 1021.
- (a) C. Zlotea, R. Campesi, F. Cuevas, E. Leroy, P. Dibandjo, C. Volkringer, T. Loiseau, G. Férey and M. Latroche, *J. Am. Chem. Soc.*, 2010, **132**, 2991; (b) J. H. Luo, H. W. Xu, Y. Liu, Y. H. Zhao, L. L. Daemen, C. Brown, T. V. Timofeeva, S. Q. Ma and H. C. Zhou, *J. Am. Chem. Soc.*, 2008, **130**, 9626; (c) X. S. Wang, S. Ma, P. M. Forster, D. Yuan, J. Eckert, J. J. López, B. J. Murphy, J. B. Parise and H. C. Zhou, *Angew. Chem., Int. Ed.*, 2008, **47**, 7263; (d) A. R. Millward and O. M. Yaghi, *J. Am. Chem. Soc.*, 2005, **127**, 17998; (e) J. L. C. Rowsell and O. M. Yaghi, *Angew. Chem., Int. Ed.*, 2005, **44**, 4670; (f) D. Sun, Y. Ke, T. M. Mattox, A. O. Betty and H. C. Zhou, *Chem. Commun.*, 2005, 5447.
- (a) W. G. Lu, L. Jiang, X. L. Feng and T. B. Lu, *Inorg. Chem.*, 2009, **48**, 6997; (b) A. P. Nelson, D. A. Parrish, L. R. Cambrea, L. C. Baldwin, N. J. Trivedi, K. L. Mulfort, O. K. Farha and J. T. Hupp, *Cryst. Growth Des.*, 2009, **9**, 4588; (c) A. Nalaparaju, R. Babarao, X. S. Zhao and J. W. Jiang, *ACS Nano*, 2009, **3**, 2563; (d) K. L. Gurunatha, S. Mohapatra, P. A. Suchetan and T. K. Maji, *Cryst. Growth Des.*, 2009, **9**, 3844; (e) J. A. Zhao, L. W. Mi, J. Y. Hu, H. W. Hou and Y. T. Fan, *J. Am. Chem. Soc.*, 2008, **130**, 15222; (f) S. A. Kozimor, B. M. Bartlett, J. D. Rinehart and J. R. Long, *J. Am. Chem. Soc.*, 2007, **129**, 10672.
- (a) X. Feng, J. S. Zhao, B. Liu, L. Y. Wang, S. Ng, G. Zhang, J. G. Wang, X. G. Shi and Y. Y. Liu, *Cryst. Growth Des.*, 2010, **10**, 1399; (b) Y. W. Lin, B. R. Jian, S. C. Huang, C. H. Huang and K. F. Hsu, *Inorg. Chem.*, 2010, **49**, 2316; (c) L. Zhang, Y. Y. Li, Z. J. Qin, Q. P. Li, J. K. Cheng, J. Zhang and Y. G. Yao, *Inorg. Chem.*, 2008, **47**, 8286; (d) C. A. Bauer, T. V. Timofeeva, T. B. Settersten, B. D. Patterson, V. H. Liu, B. A. Simmons and M. D. Allendorf, *J. Am. Chem. Soc.*, 2007, **129**, 7136.
- (a) Q. Yue, Q. Sun, A. L. Cheng and E. Q. Gao, *Cryst. Growth Des.*, 2010, **10**, 44; (b) L. Yan, Q. Yue, Q. X. Jia, G. Lemerrier and E. Q. Gao, *Cryst. Growth Des.*, 2009, **9**, 2984; (c) H. Ren, T. Y. Song, J. N. Xu, S. B. Jing, Y. Yu, P. Zhang and L. R. Zhang, *Cryst. Growth Des.*, 2009, **9**, 105; (d) X. L. Chen,

- B. Zhang, H. M. Hu, F. Fu, X. L. Wu, T. Qin, M. L. Yang, G. L. Xue and J. W. Wang, *Cryst. Growth Des.*, 2008, **8**, 3706; (e) Y. Q. Wei, Y. F. Yu and K. C. Wu, *Cryst. Growth Des.*, 2008, **8**, 2087.
- 8 (a) M. Dinca, A. F. Yu and J. R. Long, *J. Am. Chem. Soc.*, 2006, **128**, 8904; (b) C. Serre, F. Millange, C. Thouvenot, M. Nogues, G. Marsolier, D. Louer and G. Férey, *J. Am. Chem. Soc.*, 2002, **124**, 13519.
- 9 (a) J. Zhang, T. Wu, S. M. Chen, P. Y. Feng and X. H. Bu, *Angew. Chem., Int. Ed.*, 2009, **48**, 3486; (b) S. L. Xie, B. Q. Xie, X. Y. Tang, N. Wang and S. T. Yue, *Z. Anorg. Allg. Chem.*, 2008, **634**, 842; (c) C. Daiguebonne, N. Kerbellec, K. Bernot, Y. Gérault, A. Deluzet and O. Guillou, *Inorg. Chem.*, 2006, **45**, 5399; (d) T. M. Reineke, M. Eddaoudi, M. O'Keeffe and O. M. Yaghi, *Angew. Chem., Int. Ed.*, 1999, **38**, 2590.
- 10 (a) Y. H. Zhao, Z. M. Su, Y. M. Fu, K. Z. Shao, P. Li, Y. Wang, X. R. Hao, D. X. Zhu and S. D. Liu, *Polyhedron*, 2008, **27**, 583; (b) F. E. Jarrod, D. W. Rosa and E. Mohamed, *Chem. Commun.*, 2005, **16**, 2095.
- 11 (a) L. L. Wen, D. B. Dang, C. Y. Duan, Y. Z. Li, Z. F. Tian and Q. J. Meng, *Inorg. Chem.*, 2005, **44**, 7161; (b) B. Zhao, X. Y. Chen, P. Cheng, D. Z. Liao, S. P. Yan and Z. H. Jiang, *J. Am. Chem. Soc.*, 2004, **126**, 15394; (c) K. G. Suji and K. B. Parimal, *Inorg. Chem.*, 2003, **42**, 8250.
- 12 (a) H. L. Gao, L. Yi, B. Zhao, X. Q. Zhao, P. Cheng, D. Z. Liao and S. P. Yan, *Inorg. Chem.*, 2006, **45**, 5980; (b) B. Zhao, H. L. Gao, X. Y. Chen, P. Cheng, W. Shi, D. Z. Liao, S. Y. Yan and Z. H. Jiang, *Chem.–Eur. J.*, 2006, **12**, 149.
- 13 (a) B. L. Chen, K. F. Mok, S. C. Ng and G. B. D. Michael, *New J. Chem.*, 1999, **23**, 877; (b) B. L. Chen, K. F. Mok, S. C. Ng and G. B. D. Michael, *Polyhedron*, 1999, **18**, 1211; (c) W. Huang, D. Y. Wu, P. Zhou, W. B. Yan, D. Guo, C. L. Duan and Q. J. Meng, *Cryst. Growth Des.*, 2009, **9**, 1362.
- 14 (a) H. H. Li, W. Shi, N. Xu, Z. J. Zhang, Z. Niu, T. Han and P. Cheng, *Cryst. Growth Des.*, 2012, **12**, 260; (b) H. H. Li, W. Shi, K. N. Zhao, Z. Niu, H. M. Li and P. Cheng, *Chem.–Eur. J.*, 2013, **19**, 3358.
- 15 (a) Z. J. Zhang, W. Shi, Z. Niu, H. H. Li, B. Zhao, P. Cheng, D. Z. Liao and S. P. Yan, *Chem. Commun.*, 2011, **47**, 425; (b) K. L. Mulfort, O. K. Farha, C. D. Malliakas, M. G. Kanatzidis and J. T. Hupp, *Chem.–Eur. J.*, 2010, **16**, 276.
- 16 K. Baooram, B. Francis, R. Bissessur and R. Narain, *Compos. Sci. Technol.*, 2008, **68**, 617.
- 17 G. M. Sheldrick, *Acta Crystallogr., Sect. A: Found. Crystallogr.*, 2008, **64**, 112.
- 18 A. L. Spek, *Acta Crystallogr., Sect. A: Found. Crystallogr.*, 1990, **46**, C34.
- 19 S. Norbert and B. Shyam, *Chem. Rev.*, 2012, **112**, 933.
- 20 (a) S. R. Batten, B. F. Hoskins and R. Robson, *Chem.–Eur. J.*, 2000, **6**, 156; (b) S. C. Manna, A. D. Jana, G. M. Rosair, G. B. Michael, D. G. Mostafab and N. R. Chaudhuri, *J. Solid State Chem.*, 2008, **181**, 457.
- 21 (a) J. Juillard, *Pure Appl. Chem.*, 1977, **49**, 885; (b) M. Boča, I. Svoboda, F. Renz and H. Fuess, *Acta Crystallogr., Sect. C: Cryst. Struct. Commun.*, 2004, **60**, 631; (c) H. Li, W. Shi, K. Zhao, Z. Niu, X. Chen and P. Cheng, *Chem.–Eur. J.*, 2012, **18**, 5715.
- 22 (a) X. L. Zhao, J. M. Dou, D. Sun, P. P. Cui, D. F. Sun and Q. Y. Wu, *Dalton Trans.*, 2012, **41**, 1928; (b) R. Q. Zou, X. H. Bu and R. H. Zhang, *Inorg. Chem.*, 2004, **43**, 5382; (c) B. Kumar, H. Yoshito and F. Makoto, *Angew. Chem., Int. Ed.*, 2002, **41**, 3395.
- 23 V. A. Blatov, Multipurpose crystallochemical analysis with the program package TOPOS. IUCr Comp Comm Newsletter 7, 4–38, 2006; available at http://iucrcomputing.ccp14.ac.uk/iucr_top/comm/-ccom/newsletters/2006nov/.
- 24 (a) H. L. Jiang, T. A. Makal and H. C. Zhou, *Coord. Chem. Rev.*, 2013, **257**, 2232; (b) G. P. Yang, L. Hou, X. J. Luan, B. Wu and Y. Y. Wang, *Chem. Soc. Rev.*, 2012, **41**, 6992; (c) Y. Takashima, V. M. Martínez, S. Furukawa, M. Kondo, S. Shimomura, H. Uehara, M. Nakahama, K. Sugimoto and S. Kitagawa, *Nat. Commun.*, 2011, **2**, 168; (d) K. L. Mulfort, O. K. Farha, C. D. Malliakas, M. G. Kanatzidis and J. T. Hupp, *Chem.–Eur. J.*, 2010, **16**, 276; (e) M. H. Mir, S. Kitagawa and J. J. Vittal, *Inorg. Chem.*, 2008, **47**, 7728; (f) B. L. Chen, S. Ma, F. Zapata, F. R. Fronczek, E. B. Lobkovsky and H. C. Zhou, *Inorg. Chem.*, 2007, **46**, 1233.
- 25 (a) J. Y. Zou, H. L. Gao, W. Shi, J. Z. Cui and P. Cheng, *CrystEngComm*, 2013, **15**, 2682; (b) Y. J. Cui, Y. F. Yue, G. D. Qian and B. L. Chen, *Chem. Rev.*, 2012, **112**, 1126; (c) X. M. Jing, H. Meng, G. H. Li, Y. Yu, Q. S. Huo, M. Eddaoudi and Y. L. Liu, *Cryst. Growth Des.*, 2010, **10**, 3489.
- 26 (a) P. Cui, Z. Chen, D. L. Gao, B. Zhao, W. Shi and P. Cheng, *Cryst. Growth Des.*, 2010, **10**, 4370; (b) M. S. Wang, S. P. Guo, Y. Li, L. Z. Cai, J. P. Zou, G. Cu, W. W. Zhou, F. K. Zheng and G. C. Guo, *J. Am. Chem. Soc.*, 2009, **131**, 13572; (c) L. Z. Duan, H. Wu, J. P. Ma, X. W. Wu and Y. B. Dong, *Inorg. Chem.*, 2010, **49**, 11164.
- 27 (a) M. S. Wang, S. P. Guo, Y. Li, L. Z. Cai, J. P. Zou, G. Cu, W. W. Zhou, F. K. Zheng and G. C. Guo, *J. Am. Chem. Soc.*, 2009, **131**, 13572; (b) P. Cui, Z. Chen, D. L. Gao, B. Zhao, W. Shi and P. Cheng, *Cryst. Growth Des.*, 2010, **10**, 4370; (c) L. Duan, Z. H. Wu, J. P. Ma, X. W. Wu and Y. B. Dong, *Inorg. Chem.*, 2010, **49**, 11164.
- 28 (a) G. Yuan, K. Z. Shao, D. Y. Du, X. L. Wang, Z. M. Su and J. F. Ma, *CrystEngComm*, 2012, **14**, 1865; (b) L. L. Wen, Z. D. Lu, J. G. Lin, Z. F. Tian, H. Z. Zhu and Q. J. Meng, *Cryst. Growth Des.*, 2007, **7**, 93; (c) S. L. Zheng, J. H. Yang, X. L. Yu, X. M. Chen and W. T. Wong, *Inorg. Chem.*, 2004, **43**, 830.